

Flexible and Printed Electronics



PAPER

Amorphous IGZO field effect transistor based flexible chemical and biosensors for label free detection

Deepa Bhatt^{1,2}, Satyendra Kumar^{1,2,3} and Siddhartha Panda^{1,2,3,4} 

¹ Materials Science Programme, Indian Institute of Technology Kanpur, Kanpur-208016, India

² Samtel Centre for Display Technologies, Indian Institute of Technology Kanpur, Kanpur-208016, India

³ Department of Chemical Engineering, Indian Institute of Technology Kanpur, Kanpur-208016, India

⁴ National Centre for Flexible Electronics, Indian Institute of Technology Kanpur, Kanpur-208016, India

E-mail: spanda@iitk.ac.in

Keywords: electrolytic gated field effect transistor, indium gallium zinc oxide, flexible substrates, biosensor

Abstract

Flexible chemical sensors and biosensors are of interest in different industry sectors and have advantages for being shape-friendly, lightweight, with potential of low cost. The performance factors such as fast response and label free detection makes field effect transistors an attractive platform for such sensors. While there is a large body of literature on ion sensitive field effect transistors using rigid substrates, limited studies are reported on flexible substrates. Electrolytic gated field effect transistors, a class of ion sensitive field effect transistors, have a further advantage as no gate dielectrics are needed (with the electrolytic solution itself acting as the gate dielectric) and need lower operating voltages; there are no reports yet of electrolytic gated field effect transistor with amorphous indium gallium zinc oxide as the semiconductor as well as a sensing layer on flexible substrates and this is the subject of the present work, where fully flexible electrolytic gated field effect transistors are demonstrated on flexible polyethylene terephthalate substrates for pH sensing and for detection of prostate specific antigen. Bottom contact electrolytic gated field effect transistors structures with indium tin oxide as the source and drain were fabricated on flexible polyethylene terephthalate substrates with amorphous indium gallium zinc oxide as the semiconductor deposited over indium tin oxide at room temperature. Materials and electrical characterizations (in a low operating voltage range of -1 – 1.5 V) were conducted. A pH sensitivity of 20 ± 2 mV pH⁻¹ was demonstrated. Stability studies and bending tests were also conducted. Label-free bio-sensing for prostate specific antigen was demonstrated in the concentration range 1 pg ml⁻¹– 10 ng ml⁻¹ in phosphate buffer saline. This learning can be utilized to fabricate wearable sensors for healthcare monitoring at low cost.

1. Introduction

There is a need for flexible diagnostic devices in several industry sectors such as medical [1, 2], environmental [3] and food [4–6]. Field effect transistor (FET) based chemical and biosensors [7–9] are of interest because of their fast response, simple structure, direct transduction and label free detection [10–12]. While there are a large number of studies reported for ion sensitive FETs (ISFETs) [13–16] based chemical and biosensors on rigid substrates [17–19] over the past few decades, there are limited studies reported on flexible substrates [20]. Flexible chemical sensors and biosensors have advantages on account of being lightweight, having potential of low cost, and being

form-factor amenable. Fabrication of ISFETs on flexible substrates using vacuum based processes (such as PECVD, sputtering and ALD) have challenges on account of high thermal budgets associated with the deposition and the subsequent annealing of the gate dielectrics. A class of ISFETs, electrolytic gated FETs (EGFETs), have advantages on account of no requirement of gate dielectrics (with the electrolytic solution itself acting as the gate dielectric), and the low operating voltages of these devices make them suitable for point of care applications. ISFET based chemical and bio-sensors on rigid substrates have been demonstrated with different semiconductor materials such as Si, GaAs, ZnO and amorphous indium gallium zinc oxide (a-IGZO). For improving the sensitivity of FET

based sensors, 1D and 2D materials [7, 9] as the semiconductor have been investigated; however, their fabrication processes and the alignment of these materials within the source-drain region have been reported to be difficult [21]. The a-IGZO [22–24] is a suitable candidate for flexible sensors because of the room temperature deposition (low thermal budget), superior electrical properties (high mobility, high $I_{\text{on}}/I_{\text{off}}$ and low sub threshold swing) and properties suitable for applications in transparent flexible electronics [22, 25].

On rigid substrates, although there are several reports on a-IGZO based ISFETs with separate sensing layers such as SnO_2 [14, 18, 26], Ta_2O_5 [16, 27], SiO_2 [28], Al_2O_3 [29], there are very few reports [30, 31] on a-IGZO as the sensing layer as well as the semiconductor (i.e. in EGFET) [20]. There are few reports in the literature regarding EGFETs on rigid substrates with organic semiconductors [32] and graphene [33] as the sensing layers. Two classes of flexible ISFETs are reported in literature, (i) semi-flexible or flex-rigid and (ii) fully flexible. As an example of semi-flexible ISFETs [34], the sensing measurements were done on the flexible polyethylene terephthalate (PET) substrates with indium tin oxide (ITO) as the sensing layer, utilizing conventional rigid metal oxide field effect transistors (MOSFETs) (with Si as the semiconductor); as an example of fully flexible ISFETs [35], all components of the device (including the sensing region) were fabricated on flexible substrates. In this work we focus on fully flexible ISFETs. There is only one report, of a-IGZO semiconductor based ISFET on fully flexible substrates, and this has an extended gate ISFET structure [36]; and there is one report of a flexible ISFET with indium zinc-oxide (IZO) as the semiconductor and nanogranular SiO_2 (n- SiO_2) as the sensing layer [37]. To the best of our knowledge, EGFETs with a-IGZO as the semiconductor as well as a sensing layer, at low operating voltages on flexible substrates have not been reported yet and this is the subject of the present work.

In this work, simple and low cost fully flexible EGFETs were fabricated on PET substrates with a-IGZO as the sensing layer for both (i) pH sensing as well as for (ii) detection of prostate specific antigen (PSA). A bottom contact EGFET structure with ITO as the source and drain was fabricated by photolithography on PET substrates, and a-IGZO as the semiconductor was deposited over the ITO at room temperature by rf sputtering. A reservoir of size $10 \times 1 \text{ mm}^2$ was made for the sensing application on the a-IGZO surface with the help of SU 8 epoxy. Bending tests and stability tests were performed on the devices. For bio-sensing, few additional fabrication steps were effected on the same structure at room temperature by introducing a molecular stack to attach anti-PSA (polyclonal) to detect PSA [11, 38]. Fluorescence microscopy and atomic force microscopy were conducted for the validation of attachment of the antibodies on the a-IGZO surface.

2. Experiments

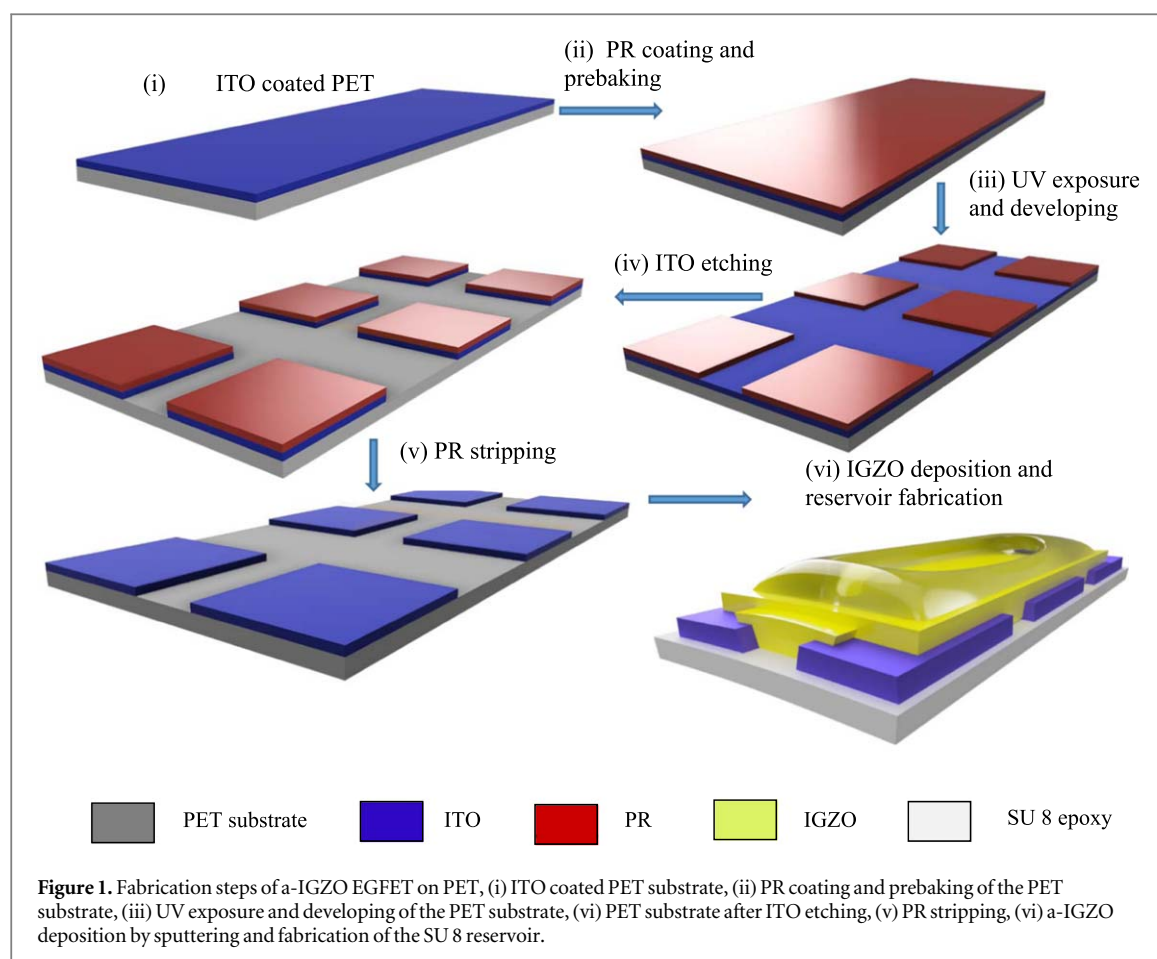
2.1. Materials

ITO coated PET substrates were purchased from Mianyang Prochema Commercial Co. Ltd (China). A sputtering target (4' diameter) for InGaZnO_4 was purchased [16, 39] from Able Target Ltd (China). The standard pH buffer solutions were purchased from Merck Millipore (India), and made from potassium hydrogen phthalate (pH 4.0), potassium dihydrogen phosphate/disodium hydrogen phosphate (pH 7.0), and boric acid/potassium chloride/sodium hydroxide (pH 9.0); and were verified by a commercial pH meter. Epoxy (SU-8 2002), photoresists (PR) 3510 and tetramethylammonium hydroxide (TMAH) solution were purchased from Microchem (USA), Allresist (Germany), and Sigma Aldrich (Germany) respectively. Materials for biosensors such as hydrogen peroxide (H_2O_2), branched polyethylenimine (BPEI), as used in our previous work [40] with average molecular weight of 60 000, anti-PSA IgG (polyclonal) and prostate-specific- antigen (PSA) were purchased from Thermo Fisher Scientific India Pvt. Ltd (India), Sigma Aldrich (Germany), Genetech Lab Biotech Park (India), and Fitzgerald (USA), respectively.

2.2. Fabrication and characterization

2.2.1. Fabrication and characterization of pH sensor

2.5 cm \times 2.5 cm ITO coated PET substrates of thickness $175 \mu\text{m}$ were used to fabricate the pH sensors. For device fabrication, the source and the drain utilizing ITO were fabricated by photolithography. We deposited 30 nm [19, 40] and 100 nm [39] amorphous indium gallium zinc oxide (a-IGZO) by rf sputtering using the deposition parameters i.e. at room temperature, rf power, as reported in our previous work. Unlike as in the previous works, here deposition pressure and the annealing temperature of the a-IGZO films were 1.0×10^{-2} mbar and 100°C , respectively. We fabricated the reservoir with SU 8 epoxy using the protocol described in our previous work [19–40]. For photolithography, initially the ITO coated PET substrates were placed on a hot plate for 10 min at 100°C (figure 1(i)), then positive PR 3510 was coated on the substrates followed by prebaking at 100°C (figure 1(ii)). The PR coated PET substrates were subjected to ultraviolet (UV) exposure for 25 s with the help of a mask aligner (Karl Suss MA 1006). The substrates were then developed by tetramethylammonium hydroxide (TMAH) solution and post-baked for 5 min at 100°C as shown in figure 1(iii). The developed substrates, were dipped in an ITO etchant for the removal of the ITO as shown in figure 1(iv). For removal of PR, the substrates were subjected to UV exposure followed by development as shown in figure 1(v). After fabrication of the source and drain electrodes, 30 nm a-IGZO as the semiconductor was deposited by sputtering at room temperature and at



9×10^{-3} mbar deposition pressure in an Ar atmosphere. Again 100 nm a-IGZO was deposited as a sensing layer on top of the semiconducting layer followed by the annealing of IGZO at 100 °C in presence of oxygen. After fabrication of the EGFET, a reservoir of $10 \times 1 \text{ mm}^2$ with epoxy (SU-8 2002) was made on top of the device by photolithography for holding the pH solutions, as shown in figure 1(vi). For the materials and electrical characterizations—x-ray diffraction (Panalytical XPert) measurements were done for the confirmation of amorphous nature of IGZO film by varying the 2θ values from 20° to 80°, and a semiconductor parameter analyzer (Agilent 1500 A) was used to measure the current voltage (IV) characteristics of the EGFET at a low voltage range (−1–1.5 V).

2.2.2. Bending experiments

The bending tests could be performed on the EGFETs by several methods [41], such as (i) wrapping the EGFET on a curved surface (the static bending test) and (ii) repetitive bends to a fixed radii on a bending machine (dynamic bending test). In this work we have performed the dynamic bending test on the EGFET using a custom-built set-up [42, 43]. The main part of the custom-build set-up consists of two rods, the upper one rotating about its axis and the lower one being stationary, as shown in figure 2(a). The EGFET

was fixed in between the two rods as shown in figure 2(b), and the upper rod was rotated a hundred times in one minute; the bending radius varied from infinity (figure 2(c)) when the films was planar and 6 mm (figure 2d) when the film was bent to the maximum. The EGFET was then removed from the set-up and flattened, and then current voltage (IV) characteristics were measured. A schematic of the device in the bent state is shown in figure 2(e). After subjecting the devices to the bending regime, the pH sensing of EGFETs were characterized by a semiconductor parameter analyzer (Agilent 1500 A) with different pH solutions.

2.2.3. Fabrication and characterization of the biosensor

For fabrication of the biosensor, few additional steps (shown in figure 3) were made on the structure used for pH sensing. These fabrication steps were similar to that used in our previous works [11, 38] with some modifications such as different concentrations of glutaraldehyde, different times for hydrosolysis, amine attachemt and crosslinking of H_2O_2 , BPEI and glutaraldehyde, and different amounts (5 μl) of each of the chemicals used for the immobilization processes. In step 1, the EGFET was treated with 10% H_2O_2 solution in Millipore deionised (DI) water for 1 h to hydrolyze the surface and then washed with DI as shown in figure 3(a). In step 2, the EGFET was treated with 0.5%

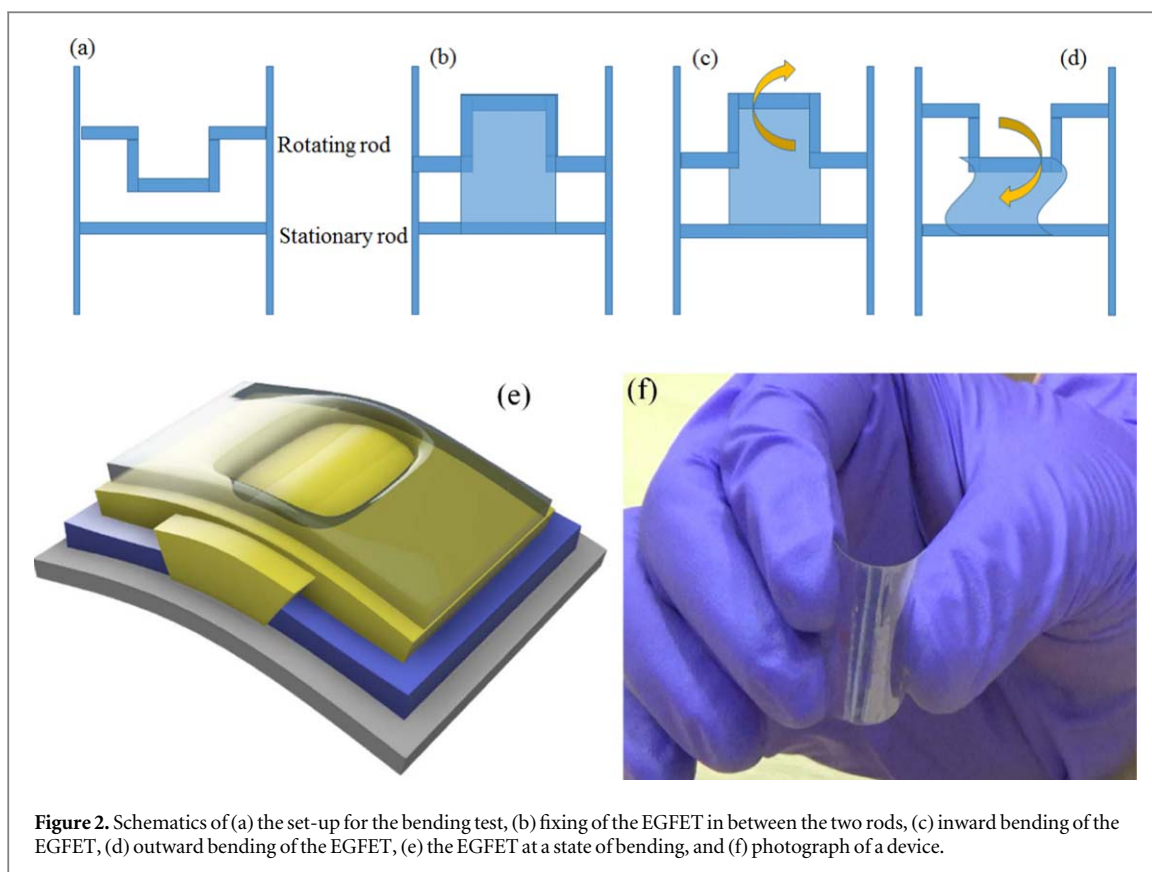


Figure 2. Schematics of (a) the set-up for the bending test, (b) fixing of the EGFET in between the two rods, (c) inward bending of the EGFET, (d) outward bending of the EGFET, (e) the EGFET at a state of bending, and (f) photograph of a device.

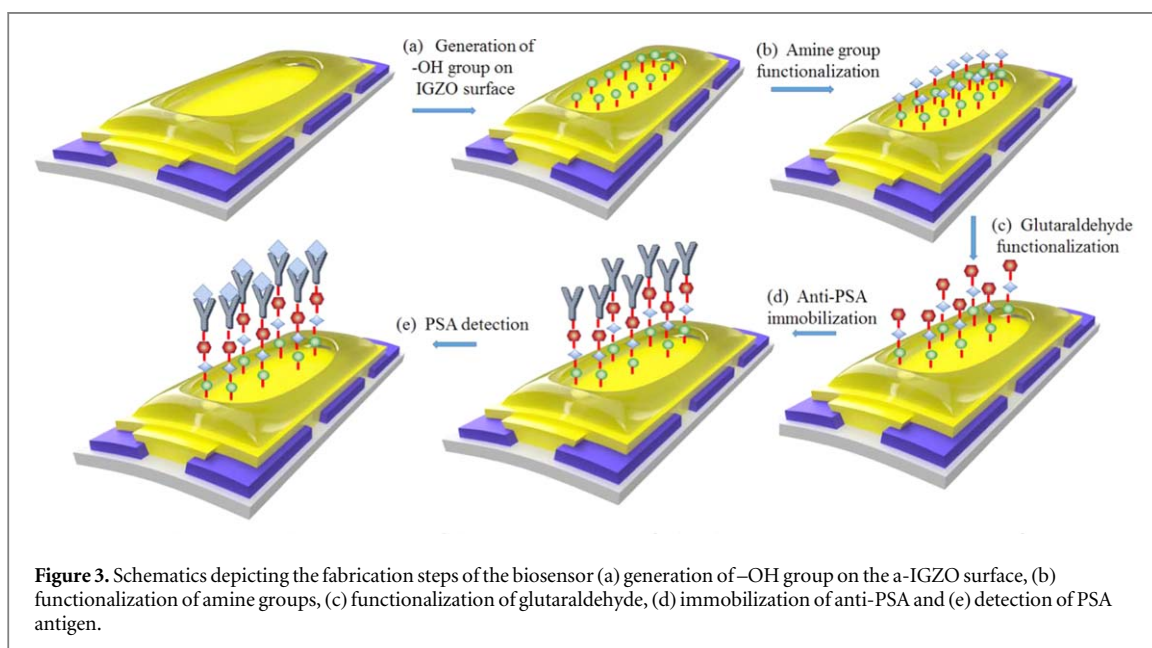


Figure 3. Schematics depicting the fabrication steps of the biosensor (a) generation of $-OH$ group on the a-IGZO surface, (b) functionalization of amine groups, (c) functionalization of glutaraldehyde, (d) immobilization of anti-PSA and (e) detection of PSA antigen.

of BPEI for 3 h for functionalization of the amine group as shown in figure 3(b). In step 3, 2.5% of glutaraldehyde in DI water was functionalized on the reservoir of the EGFET for 1 h to immobilize the anti-PSA IgG (polyclonal), as shown in figure 3(c). Finally in step 4, 0.1 mg ml^{-1} anti-PSA IgG (polyclonal) solution in phosphate buffer solution (PBS) was drop casted on the reservoir of the EGFET (shown in figure 3(d)) followed by keeping the substrate in an incubator for 16 h at 4°C for the immobilization of

the antibodies. For detection of PSA, $2 \mu\text{l}$ of PSA was kept on the antibody immobilized EGFET surface with concentrations ranging from 1 pg ml^{-1} to 10 ng ml^{-1} and the sensor surface was rinsed with phosphate buffer solution (PBS) to remove the adsorbed antigen and then dried with N_2 gas figure 3(e) shows the schematic of PSA bound with the anti-PSA.

Atomic force microscope imaging (AFM) (Atomic Force Microscope Oxford Instruments, USA) in the tapping mode and fluorescence microscope imaging

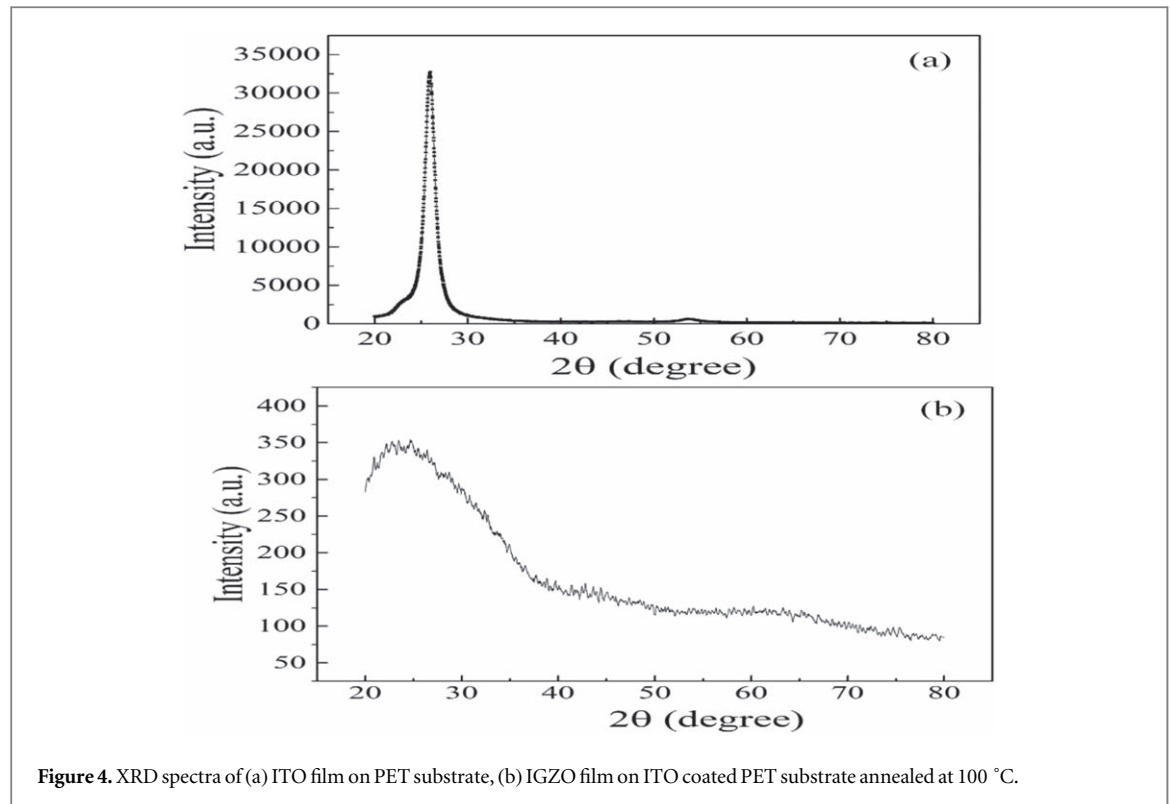


Figure 4. XRD spectra of (a) ITO film on PET substrate, (b) IGZO film on ITO coated PET substrate annealed at 100 °C.

(Fluorescence Microsystem, Leica Micro-systems, Germany) at a wavelength of 494 nm were done for the validation of immobilization of the antibodies on the a-IGZO surface. For fluorescence microscopy, 0.1 mg ml⁻¹ solution of anti-PSA IgG tagged with Fluorescein isothiocyanate (FITC) in PBS was immobilized on the reservoir. Again, a semiconductor parameter analyzer (Agilent 1500 A) was used to measure the current voltage (*IV*) characteristics of the EGFET for detection of the captured antigen.

3. Results and discussion

3.1. Material characterization for pH sensors

3.1.1. X-ray diffraction and atomic force microscopy

Figure 4(a) and (b) present the XRD spectra of ITO coated PET substrate and the a-IGZO film on the ITO coated PET substrate, respectively. A sharp peak at 25° seen in figure 4(a) is attributed to the (222) plane of ITO [44, 45]. The amorphous nature of the IGZO film is evident from the spectra seen in figure 4(b).

Root mean square (RMS) roughness of 3 nm was observed on the ITO coated PET sheets (figure 5(a)), and while figure 5(b) depicts the surface morphology of the a-IGZO film, and a n RMS roughness of 4 nm was observed for the a-IGZO films (figure 5(b)). The RMS roughness of the a-IGZO film observed here is comparable to that observed for a-IGZO films on glass substrates (4.5 nm) [46].

3.2. Material characterization for bio-sensors

3.2.1. Atomic force microscopy and fluorescence microscopy

AFM was used to observe the attachment of FITC tagged antibodies on the a-IGZO surface. The tagged Y shaped antibodies on the a-IGZO surface are seen in figure 5(c). The RMS roughness of the antibody coated surface is 16 nm (figure 5(c)), which also confirms the attachment of the antibody on the a-IGZO surface [11].

Fluorescence microscopy was done to check the antibody immobilization on the a-IGZO surface as shown in figure 6. The FITC molecules which were excited by the photons of wave length 494 nm and emitted at 528 nm, confirmed the immobilization of antibodies [11, 47] on the a-IGZO surface.

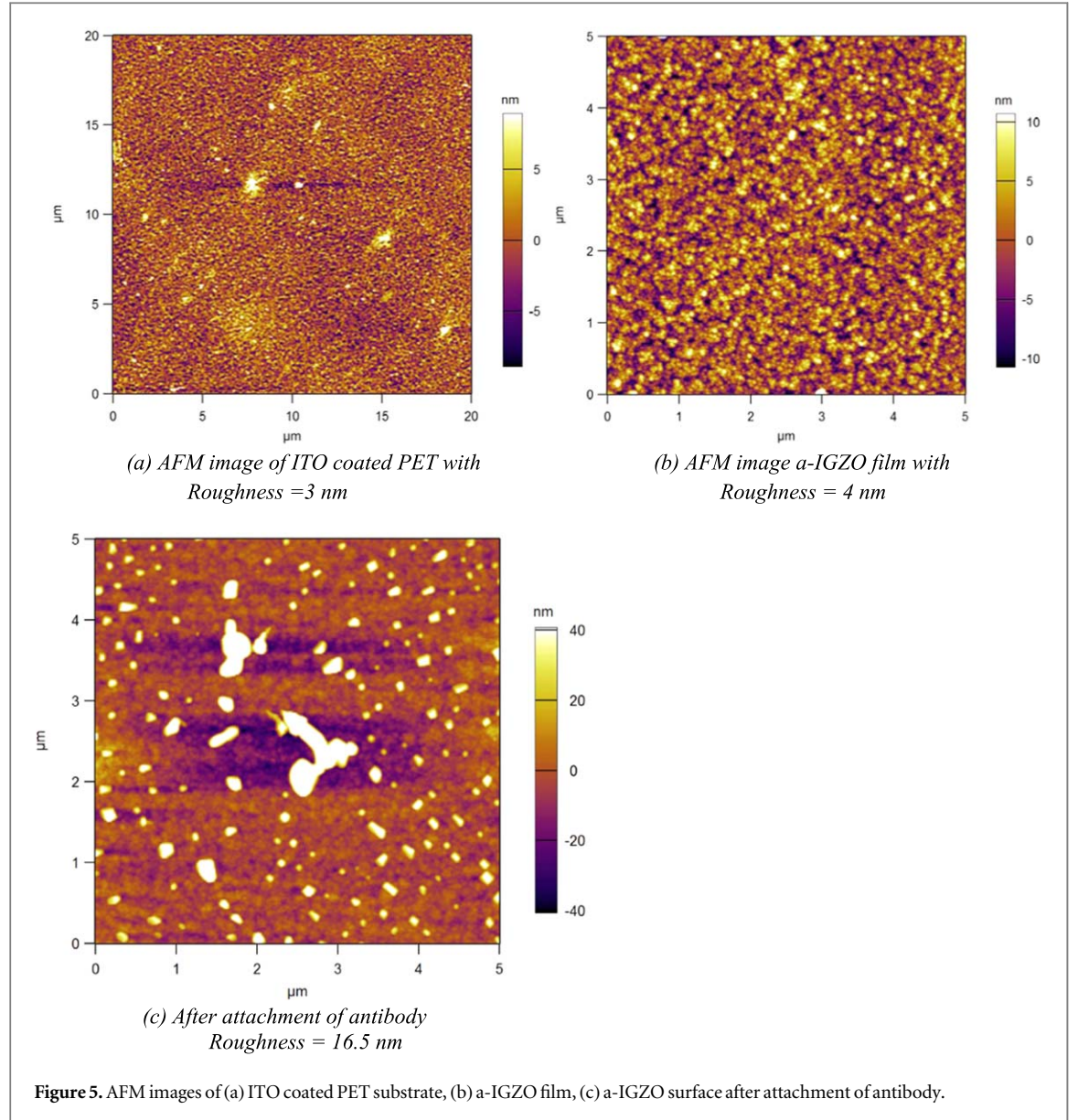
3.3. Electrical characterization of the pH sensor and the bio-sensor

The expression of the drain current (I_{DS}) [30] for the TFT and the EGFET is provided by the equation below

$$I_{DS} = \mu_{FE} C_{ox} \frac{W}{L} (V_G - V_{TH}) V_{DS}, \quad (1)$$

where μ_{FE} is the field effect mobility, C_{ox} is the capacitance of the dielectric, V_G is the gate voltage, V_{TH} is the threshold voltage, V_{DS} is the drain to source voltage, W and L are the width and the length of the channel, respectively.

In case of the EGFET, the threshold voltage of the device was determined by the surface potential, ψ , which is generated when the electrolytic solution comes in



contact with the a-IGZO surface. The expression of the threshold voltage is given by the equation [13, 30]

$$V_{TH} = E_{ref} - \Psi + \chi^{sol} - \frac{\Phi}{q} - \frac{Q_{ox}}{C_{ox}} + 2\phi_F, \quad (2)$$

where E_{ref} is the potential of reference electrode, χ^{sol} is surface dipole potential of electrolyte, Φ is work function of a-IGZO, q is unit charge, Q_{ox} is combination of charges on the a-IGZO surface and the depletion charges, and ϕ_F is the Fermi potential. In the above equation, all the parameters are constant except ψ ; thus a change in the threshold voltage depends only on ψ , and ψ is fixed for a given pH solution and changes with the change in the pH (from 4 to 9 here).

3.3.1. pH sensing characteristics of the EGFET

The EGFET was operated at a low operating voltage from -1 to 1.5 V at a constant drain voltage of 500 mV. A positive shift in the gate voltage was observed when the pH varied from 4 to 9 as shown in

figure 7(a). In the EG FET, the protonation and deprotonation [48] occurs at the a-IGZO surface when the electrolytic solution comes in contact with it. Depending on the concentration of the generated H^+ ions, the corresponding positive gate voltage acts on the a-IGZO surface, which causes increase in the drain current as a function of gate voltage as shown in figure 7(a). As the pH value is increased from 4 to 9, the H^+ concentration decreased, and a higher voltage is needed to turn on the device resulting in an increased V_{TH} . The change in the surface potential on application of the charges, generated by the electrolytic solution is given by the following equations [13, 49]

$$\frac{d\Psi}{dpH} = -2.3\alpha \left(\frac{kT}{q} \right), \quad (3)$$

where α is the sensitivity parameter and is expressed as

$$\alpha = \left(\frac{2.3kT}{q^2} \frac{C_s}{\beta_s} + 1 \right)^{-1}, \quad (4)$$

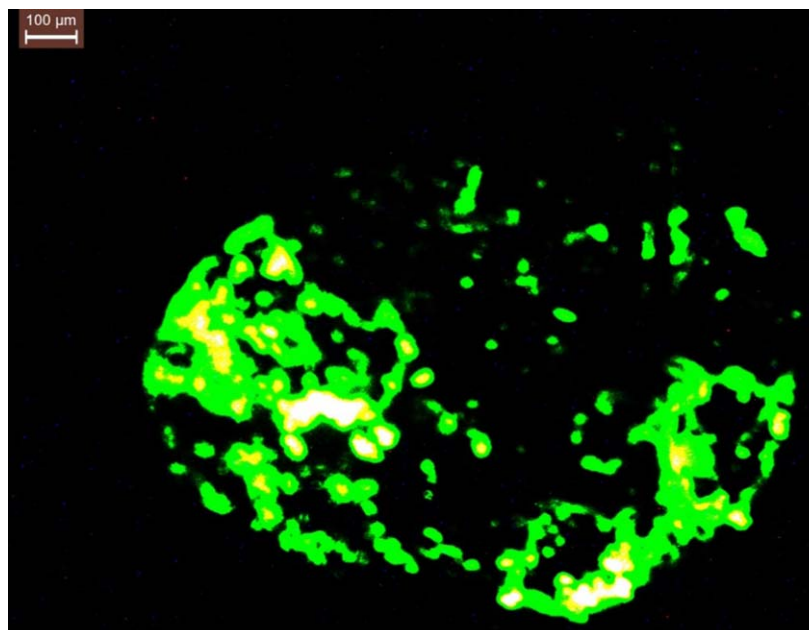


Figure 6. Fluorescence image of FITC tagged antibody.

where k , T , C_s and β_s represent the Boltzmann constant, temperature, surface capacitance, and surface buffer capacity [50, 51] respectively.

A pH sensitivity of $20 \pm 2 \text{ mV pH}^{-1}$ (based on 3 devices) is obtained here, and the sensing characteristics of one such device is shown in figure 7(a). As mentioned, there are no other reports on EGFETs on flexible substrates, hence we benchmark our results with rigid EGFETs and with flexible ISFETs. For rigid EGFETs on Si/SiO₂ substrates, pH sensitivities of 24 mV pH^{-1} [40] and 32 mV pH^{-1} [30] with a-IGZO, and 26 mV pH^{-1} [33] with graphene as the semiconducting/sensing layer have been reported. For flexible ISFETs on PET substrates, sensitivities of 37 mV pH^{-1} [52] with IZO as the semiconductor, and 50 mV pH^{-1} [53] with a-IGZO as the semiconductor, both having extended gate structures have been reported; and on polyimide (PI) substrate with a-IGZO as the semiconductor, sensitivity of 51 mV pH^{-1} [20] has been reported. Recently, sensitivity of 55 mV pH^{-1} [54] has been reported for flex-rigid ISFET on cellulose paper with an extended gate structure.

3.3.2. Stability and bending of EGFETs

To characterize the stability of the devices, we have tested the EGFET after 7 months of fabrication by keeping it in ambient conditions. A small change in the V_{TH} from 1.0 to 1.3 V, and change in I_{OFF} from 1.3×10^{-8} to $4.3 \times 10^{-10} \text{ A}$ as shown in figure 7(b), was observed after 7 months. We tried to understand this behavior from previous related studies. Exposure of a-IGZO TFT to dry ambient resulted in decreased V_{TH} accompanied by increased I_{OFF} , and this was attributed to the increase in the charge carriers due to the decrease in the oxygen-vacancies which acts as

donor-like states [55]; exposure of a-IGZO TFT to humidity resulted in increased V_{TH} accompanied by decreased I_{OFF} , and this was attributed to the decrease in the charge carriers due to the increase in the acceptor-like states caused by the water molecules [56]. In our case, the humidity in the air could be one of the reason for the observed behavior. Figure 7(c) shows the transfer characteristics of the EGFET at pH 7 before and after the bending test. Before bending, the I_{ON}/I_{OFF} of the TFT was 4.6×10^3 and after bending, it decreased to 7.3×10^2 , but still demonstrated the TFT characteristics. As mentioned, there are no reports on flexible EGFETs, and there are very limited reports of bending tests on ISFETs; in one report, Liu *et al* [52], found no change in the TFT characteristic after static bending where the device was wrapped on a cylindrical surface of radius 1.0 cm (i.e. a bending radius of 1.0 cm) and the current voltage (I – V) characteristics were measured, while in our case we performed dynamic bending with the help of custom-built set-up with bending radii 6 mm.

3.3.3. Bio-sensing characteristics

The objective of this part of the study was label free detection of PSA by the EGFET at a low operating voltage (-1 – 1.5 V). PSA concentrations of 3 – 4 ng ml^{-1} have been reported to be threshold for prostate cancer [57]. In this work, studies on the detection of PSA in the concentration range 1 pg ml^{-1} – 10 ng ml^{-1} in PBS were conducted. The drain current in the EGFET was investigated before the immobilization of anti-PSA, after the immobilization of anti-PSA, and after binding of PSA (10 ng ml^{-1} in buffer solution) with the anti-PSA. In the bare device, a lower I_{OFF} ($4.8 \times 10^{-10} \text{ A}$) was observed

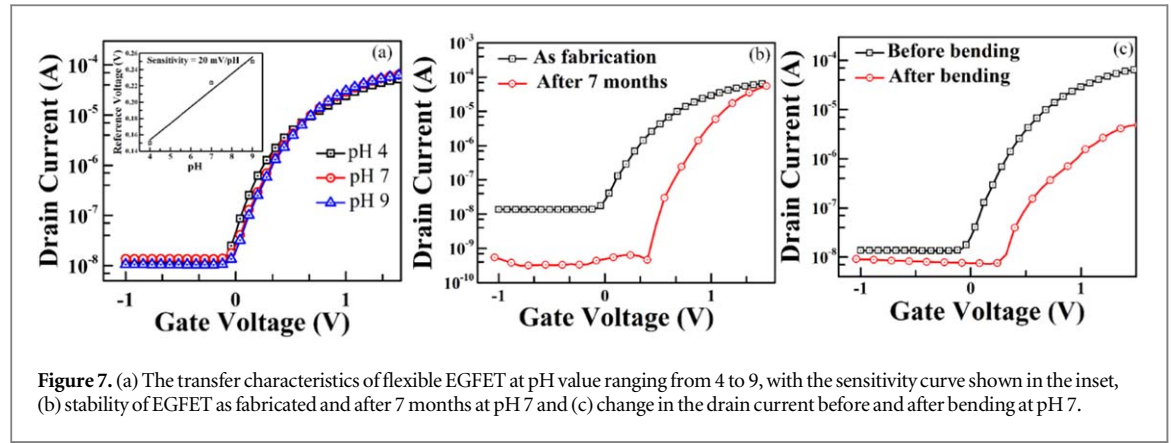


Figure 7. (a) The transfer characteristics of flexible EGFET at pH value ranging from 4 to 9, with the sensitivity curve shown in the inset, (b) stability of EGFET as fabricated and after 7 months at pH 7 and (c) change in the drain current before and after bending at pH 7.

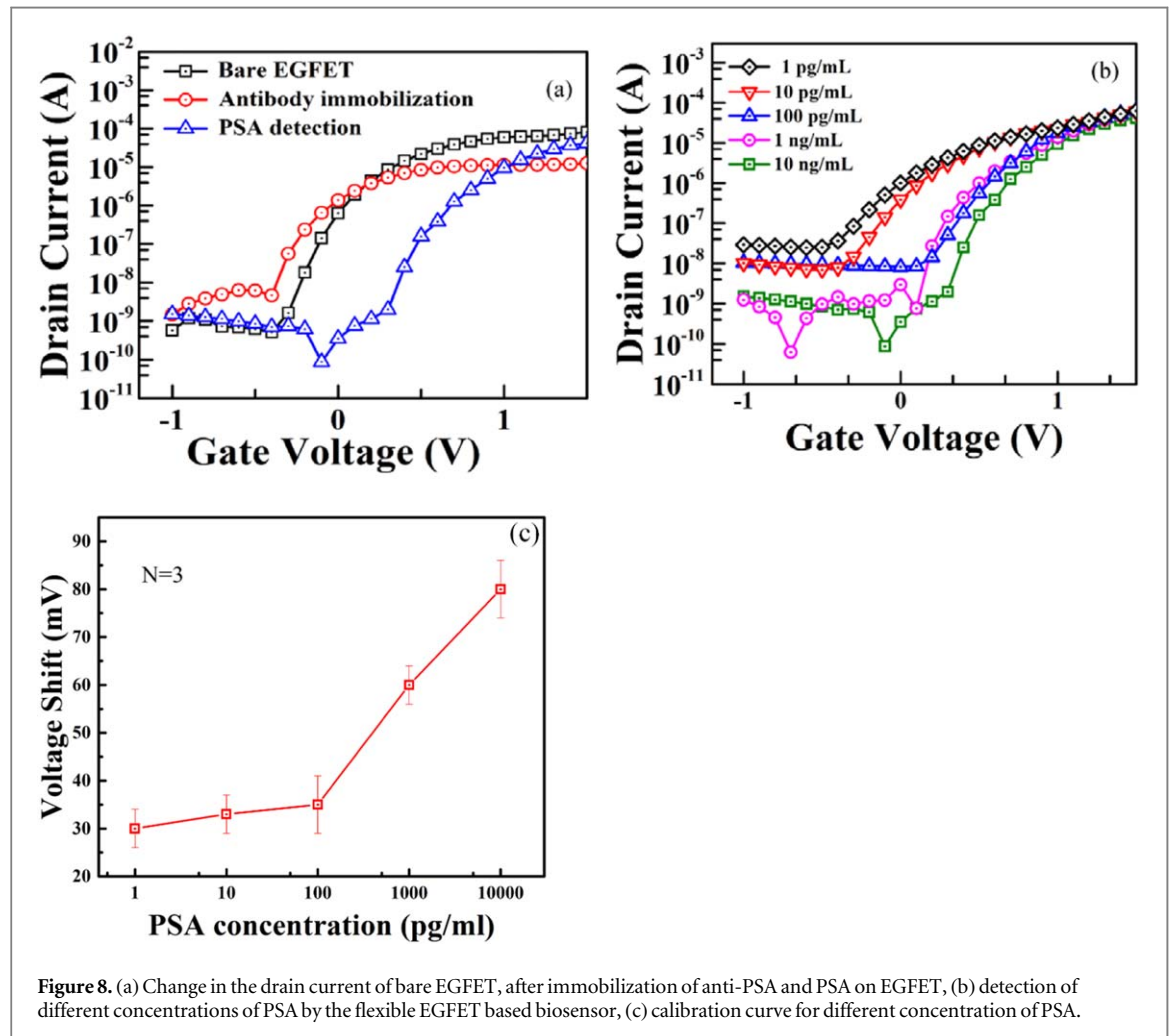


Figure 8. (a) Change in the drain current of bare EGFET, after immobilization of anti-PSA and PSA on EGFET, (b) detection of different concentrations of PSA by the flexible EGFET based biosensor, (c) calibration curve for different concentration of PSA.

which increased (4.6×10^{-9} A) after the attachment of anti-PSA, and this is attributed to the accumulation of higher negative charges inside the a-IGZO channel; a similar trend was observed by Reyes *et al* [58] in a ZnO based immunosensor where the epidermal growth factor receptor (EGFR) protein was used. PSA is usually a negatively charged molecule [59] thus when it is attached with anti-PSA, a slightly positive charge is generated at the a-IGZO surface because of the electrostatic interaction (non-covalent bonding) of the antigen-antibody pair [11]. Thus after the binding

of PSA with anti-PSA, the I_{OFF} was further decreased (5.9×10^{-10} A) as shown in figure 8(a).

The detection of PSA in the concentrations 1 pg ml^{-1} to 10 ng ml^{-1} in PBS were tested and the IV curves are shown in figure 8(b). It is observed that as the concentration of the PSA antigen increased from 1 pg ml^{-1} to 10 ng ml^{-1} , the V_{TH} of device increased and the I_{OFF} of the device decreased. As the PSA concentration increased, the negative charges inside the a-IGZO channel decreased because of the decrease in the effective positive voltage at the a-IGZO surface, resulting in higher

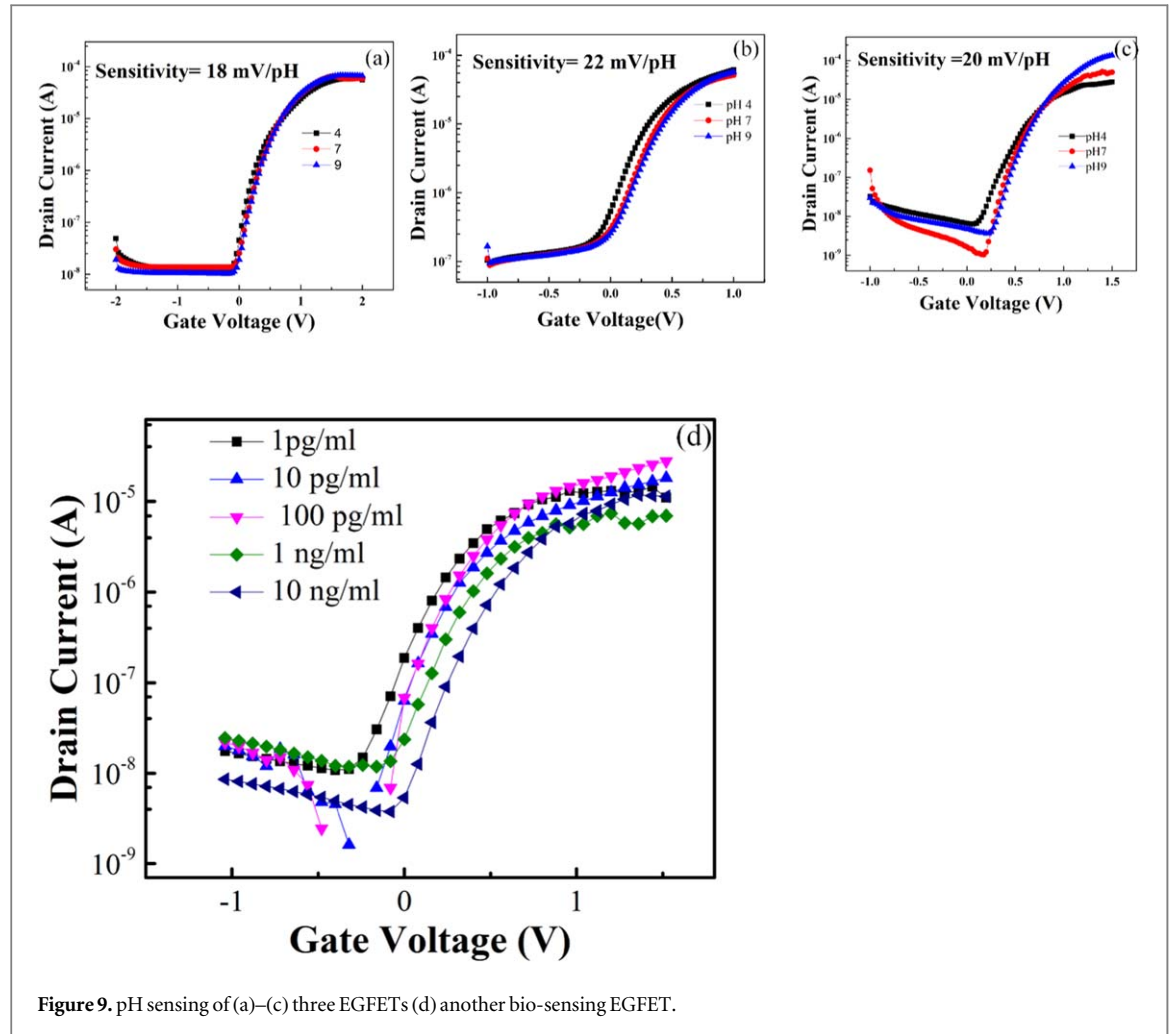


Figure 9. pH sensing of (a)–(c) three EGFETs (d) another bio-sensing EGFET.

V_{TH} and decrease in I_{OFF} . Similar trends in the IV characteristics and a comparable limit of detection ($\sim 6 \text{ pg ml}^{-1}$) [8, 11] were obtained for PSA detection in a dual-gate TFT device with MoS_2 as the semiconductor on Si/SiO_2 substrate [59], and with a silicon nanowire based FET [60, 61]. In the calibration curve the voltage shift with the concentration of PSA is shown in figure 8(c). There are two slopes in figure 8(c)—one of about 2.5 mV dec^{-1} for the PSA concentration range of $1\text{--}100 \text{ pg ml}^{-1}$ and other being about 22.5 mV dec^{-1} for the PSA concentration range of $100\text{--}10\,000 \text{ pg ml}^{-1}$.

3.3.4. Reproducibility of EGFET

We tested the reproducibility of the process for making the devices for both pH sensing and bio-sensing. Three EGFETs fabricated under identical conditions provided pH sensitivities of 18 mV/pH , 22 mV/pH and 20 mV/pH as shown in figures 9(a)–(c). For PSA detection, we have fabricated one more EGFET biosensor and found the same trend in the transfer characteristics such as (V_{TH} increasing and I_{OFF} decreasing with increasing in the PSA concentration ($1 \text{ pg ml}^{-1}\text{--}10 \text{ ng ml}^{-1}$) as shown in figure 9(d). These devices were best used for a one time measurement only.

As mentioned in the introduction section, in the literature there are no reports on EGFET based chemical

and biosensor on flexible substrates, there are a few reports on ISFET for chemical and bio-sensing on flexible substrates, and there is only one report of EGFET on rigid substrates. In table 1, we have compared the device structures, materials used, and the sensitivity of other flexible ISFETs with our work.

4. Conclusions

In this study, we have demonstrated a-IGZO based flexible EGFETs on flexible PET substrates as pH sensors and as label-free biosensors for the first time. IGZO was used as semiconductor/sensing layer with ITO as the source and drain electrodes. Materials and electrical characterizations of the devices were conducted. pH sensitivities of $20 \pm 2 \text{ mV pH}^{-1}$ were obtained. Further improvement in the sensitivities could be obtained by using different materials (e.g. 2D) and device structures (e.g. dual gate) which are a subject of future work. The stability of the devices was tested by comparing the test parameters after 7 months of storage in the ambient. A slight increase in V_{TH} ($1.0\text{--}1.3 \text{ V}$) and a decrease in I_{OFF} (1.3×10^{-8} to $4.3 \times 10^{-10} \text{ A}$) was attributed to the role of moisture. Dynamic bending tests (100 repetitions in a minute of varying the radius between infinity and 6 mm) were performed and the device showed TFT

Table 1. Comparison of ISFET based chemical sensor and bio-sensors on flexible substrate and EGFET based chemical and bio-sensor on rigid substrates.

S.N.	References	Structure	Substrate	Semiconductor	Performance	
					Sensitivity (mV/pH)	Detection range of bio-sensor
1	Nakata <i>et al</i> [20]	ISFET with extended gate	Flexible (PI)	IGZO	51	1–80 mM
2	Bhat <i>et al</i> [35]		Flexible (PET)	Si	—	
3	Lue <i>et al</i> [62]			Si	50	
4	Smith <i>et al</i> [36]			IGZO	50	
5	Liu <i>et al</i> [37]			IGZO	37	
6	Lee <i>et al</i> [59]	Rigid		MoS ₂	—	For human IgG 100 $\mu\text{g ml}^{-1}$ –10 fg ml^{-1}
7	Huang <i>et al</i> [61]			polySi nanowire	—	For PSA 1 pg ml^{-1} –10 ng ml^{-1}
8	Chae <i>et al</i> [30]			IGZO	32	For PSA –5 fg ml^{-1} –500 fg ml^{-1}
9	This work	EGFET	Flexible (PET)	IGZO	20	For alpha-synuclein (αS) proteins –10 fg ml^{-1} –1 ng ml^{-1} For PSA 1 pg ml^{-1} –10 ng ml^{-1}

characteristics with a reduced I_{ON}/I_{OFF} (4.6×10^3 to 7.3×10^2) after the test. The use of thinner substrates and other substrate materials for improved bending performance is a subject of future work. As a biosensor, PSA detection of concentrations ranging from 1 pg ml^{-1} to 10 ng ml^{-1} was demonstrated.

Acknowledgments

The financial support of the Ministry of Electronics and Information Technology, Government of India (Grant number 2(4)/2014-PEGD (IPIIW)) is acknowledged.

ORCID iDs

Siddhartha Panda  <https://orcid.org/0000-0001-9131-4264>

References

- [1] Kato Y, Ozawa S, Miyamoto C, Maehata Y, Suzuki A, Maeda T and Baba Y 2013 Acidic extracellular microenvironment and cancer *Cancer Cell Int.* **13** 89
- [2] Wojtkowiak J W, Rothberg J M, Kumar V, Schramm K J, Haller E, Proemsey J B, Lloyd M C, Sloane B F and Gillies R J 2012 Chronic Autophagy is a cellular adaptation to tumor acidic pH microenvironments *Cancer Res.* **72** 3938
- [3] Jorquera C J, Orozco J and Baldi A 2010 ISFET based microsenors for environmental monitoring *Sensors* **10** 61–83
- [4] Schaertel B J and Firstenberg-eden R 1988 Biosensors in the food industry: present and future *J. Food Prot.* **51** 811–20
- [5] Escuder-Gilabert L and Peris M 2010 Review: Highlights in recent applications of electronic tongues in food analysis *Anal. Chim. Acta* **665** 15–25
- [6] Kress-Rogers E 1991 Solid-state pH sensors for food applications *Trends Food Sci. Technol.* **2** 320–4
- [7] Sha R, Vishnu N and Badhulika S 2019 MoS₂ based ultra-low-cost, flexible, non-enzymatic and non-invasive electrochemical sensor for highly selective detection of uric acid in human urine samples *Sensors Actuators B* **279** 53–60
- [8] Deepika J, Sha R and Badhulika S 2019 A ruthenium(IV) disulfide based non-enzymatic sensor for selective and sensitive amperometric determination of dopamine *Microchim. Acta* **186** 1–10
- [9] Sha R, Komori K and Badhulika S 2017 Amperometric pH sensor based on graphene–polyaniline composite *IEEE Sens. J.* **17** 5038–43
- [10] Stern E, Klemic J F, Routenberg D A, Wyrembak P N, Turner-Evans D B, Hamilton A D, LaVan D A, Fahmy T M and Reed M A 2007 Label-free immunodetection with CMOS-compatible semiconducting nanowires *Nature* **445** 519–22
- [11] Kumar N, Kumar S, Kumar J and Panda S 2017 Investigation of mechanisms involved in the enhanced label free detection of prostate cancer biomarkers using field effect devices *J. Electrochem. Soc.* **164** B409–16
- [12] Veigas B, Fortunato E and Baptista P V Field effect sensors for nucleic acid detection: recent advances and future perspectives *Sensors* **15** 10380–98
- [13] Bergveld P 2003 Thirty years of ISFETOLOGY *Sensors Actuators B* **88** 1–20
- [14] Pyo J Y and Cho W J 2017 High-performance SEGISFET pH Sensor using the structure of double-gate α -IGZO TFTs with engineered gate oxides *Semicond. Sci. Technol.* **32** 035015
- [15] Lu C H, Hou T H and Pan T M 2018 High-performance double-gate α -InGaZnO ISFET pH Sensor using a HfO₂ gate dielectric *IEEE Trans. Electron Devices* **65** 237–42
- [16] Kumar N, Sutradhar M, Kumar J and Panda S 2017 Role of deposition and annealing of the top gate dielectric in α -IGZO TFT-based dual-gate ion-sensitive field-effect transistors *Semicond. Sci. Technol.* **32** 035013
- [17] Takechi K, Iwamatsu S, Yahagi T, Abe Y, Kobayashi S and Tanabe H 2014 Sensitivity evaluation on amorphous InGaZnO₄ thin-film transistor pH Sensors having various capacitances of ion-sensitive and bottom-gate insulators, *ECS J. Solid State Sci. Technol.* **3** Q3076–80
- [18] Ahn M J, Lim C M and Cho W J 2017 Highly sensitive ion-sensitive field-effect transistor sensor using fully transparent amorphous In–Ga–Zn–O thin-film transistors *Semicond. Sci. Technol.* **32** 035003
- [19] Bhatt D, Kumar N and Panda S 2019 Stacked top gate dielectrics in dual gate ion sensitive field effect transistors: Role of Interfaces *ACS Appl. Electron. Mater.* **1** 1465–73
- [20] Nakata S, Arie T, Akita S and Takei K 2017 Wearable, flexible, and multifunctional healthcare device with an ISFET chemical sensor for simultaneous sweat pH and skin temperature monitoring *ACS Sens.* **2** 443–8
- [21] Myung S, Solanki A, Kim C, Park J, Kim K S and Lee K-B 2011 Graphene-encapsulated nanoparticle-based biosensor for the selective detection of cancer biomarkers *Adv. Mater.* **23** 2221–5
- [22] Nomura K, Ohta H, Takagi A, Kamiya T, Hirano M and Hosono H 2004 Room-temperature fabrication of transparent flexible thin-film transistors using amorphous oxide semiconductors *Nature* **432** 488–92
- [23] Fortunato E, Barquinha P and Martins R 2012 Oxide semiconductor thin-film transistors: a review of recent advances *Adv. Mater.* **24** 2945–86
- [24] Park J S, Jeong J K, Mo Y G and Kim H D 2007 Improvements in the device characteristics of amorphous indium gallium zinc oxide thin-film transistors by Ar plasma treatment *Appl. Phys. Lett.* **90** 262106
- [25] Kumaresan Y, Lee R, Lim N, Pak Y, Kim H, Kim W and Jung G Y 2018 Extremely flexible indium-gallium-zinc oxide (IGZO) based electronic devices placed on an ultrathin poly (Methyl Methacrylate) (PMMA) substrate *Adv. Electron. Mater.* **4** 1800167
- [26] Pyo J-Y and Cho W-J 2018 In-plane-gate α -IGZO thin-film transistor for high-sensitivity pH sensor applications *Sensors Actuators B* **276** 101–6
- [27] Takechi K, Iwamatsu S, Yahagi T, Abe Y, Kobayashi S and Tanabe H 2014 Bottom-gate amorphous InGaZnO₄ thin-film transistor pH sensors utilizing top-gate effects *Japan. J. Appl. Phys.* **53** 076702
- [28] Schöning M J, Simonis A, Ruge C, Ecken H, Veggian M M and Lüth H 2002 A (Bio-) chemical field-effect sensor with macroporous Si as substrate material and a SiO₂ / LPCVD-Si₃N₄ double layer as pH transducer *Sensors* **2** 11–22
- [29] Bae T-E, Jang H-J, Lee S W and Cho W-J 2013 Enhanced sensing properties by dual-gate ion-sensitive field-effect transistor using the solution-processed Al₂O₃ sensing membranes *Japan. J. Appl. Phys.* **52** 06GK03
- [30] Chae M S, Park J H, Son H W, Hwang K S and Kim T G 2018 IGZO-based electrolyte-gated field-effect transistor for in situ biological sensing platform *Sensors Actuators B* **262** 876–83
- [31] Park S, Lee S Y, Kim C H, Lee I, Lee W J, Kim S, Lee B G, Jang J H and Yoon M H 2015 Sub-0.5 V highly stable aqueous salt gated metal oxide electronics *Sci. Rep.* **5** 13088
- [32] Buth F, Kumar D, Stutzmann M and Garrido J A 2011 Electrolyte-gated organic field-effect transistors for sensing applications *Appl. Phys. Lett.* **98** 153302
- [33] Ohno Y, Maehashi K, Yamashiro Y and Matsumoto K 2009 Electrolyte-aated graphene field-effect transistors for detecting pH and protein adsorption *Nano Lett.* **9** 3318–22
- [34] Lue C E, Wang I S, Huang C H, Shiao Y T, Wang H C, Yang C M, Hsu S H, Chang C Y, Wang W and Lai C S 2012 pH sensing reliability of flexible ITO/PET electrodes on EGFETs prepared by a roll-to-roll process *Microelectron. Reliab.* **52** 1651–4

- [35] Bhat K S, Ahmad R, Yoo J Y and Hahn Y B 2017 Nozzle-jet printed flexible field-effect transistor biosensor for high performance glucose detection *J. Colloid Interface Sci.* **506** 188–96
- [36] Shah S, Smith J, Stowell J and Christen J B 2015 Biosensing platform on a flexible substrate *Sensors Actuators B* **210** 197–203
- [37] Liu N, Zhu L Q, Feng P, Wan C J, Liu Y H, Shi Y and Wan Q 2015 Flexible sensory platform based on oxide-based neuromorphic transistors *Sci. Rep.* **5** 1–9
- [38] Kumar S, Ch R, Rath D and Panda S 2011 Densities and orientations of antibodies on nano-textured silicon surfaces *Mater. Sci. Eng. C* **31** 370–6
- [39] Kumar N, Kumar J and Panda S 2016 Back-channel electrolyte-gated a-IGZO dual-gate thin-film transistor for enhancement of pH sensitivity over nernst limit *IEEE Electron Device Lett.* **37** 500–3
- [40] Kumar N, Kumar J and Panda S 2016 Enhanced pH sensitivity over the Nernst limit of electrolyte gated a-IGZO thin film transistor using branched polyethylenimine *RSC Adv.* **6** 10810–5
- [41] Sheng J, Jeong H J, Han K L, Hong T and Park J S 2017 Review of recent advances in flexible oxide semiconductor thin-film transistors *J. Inf. Disp.* **18** 159–72
- [42] Singh D, Deepak and Garg A 2016 The combined effect of mechanical strain and electric field cycling on the ferroelectric performance of P(VDF-TrFE) thin films on flexible substrates and underlying mechanisms *Phys. Chem. Chem. Phys.* **18** 29478–85
- [43] Singh D, Choudhary A and Garg A 2018 Flexible and robust piezoelectric polymer nanocomposites based energy harvesters *ACS Appl. Mater. Interfaces* **10** 2793–800
- [44] Thirumoorathi M and Prakash J T J 2016 Structure, optical and electrical properties of indium tin oxide ultrathin films prepared by jet nebulizer spray pyrolysis technique *J. Asian Ceram. Soc.* **4** 124–32
- [45] Ghorannevis Z, Akbarnejad E and Ghorannevis M 2015 Structural and morphological properties of ITO thin films grown by magnetron sputtering *J. Theor. Appl. Phys.* **9** 285–90
- [46] Hsu C M, Tzou W C, Yang C F and Liou Y J 2015 Investigation of the high mobility IGZO thin films by using co-sputtering method *Materials* **8** 2769–81
- [47] Shen Y C, Yang C H, Chen S W, Wu S H, Yang T L and Huang J J 2014 IGZO thin film transistor biosensors functionalized with ZnO nanorods and antibodies *Biosens. Bioelectron.* **54** 306–10
- [48] Sarkar D, Liu W, Xie X, Anselmo A C, Mitragotri S and Banerjee K 2014 MoS₂ field-effect transistor for next-generation label-free biosensors *ACS Nano* **8** 3992–4003
- [49] Yan F, Estrela P, Mo Y, Migliorato P, Maeda H, Inoue S and Shimoda T 2005 Polycrystalline silicon ion sensitive field effect transistors *Appl. Phys. Lett.* **86** 053901
- [50] Bergveld P, Van Hal R E G and Eijkel J C T 1995 The remarkable similarity between the acid-base properties of ISFETs and proteins and the consequences for the design of ISFET biosensors *Biosens. Bioelectron.* **10** 405–14
- [51] Vekrellis K, Xilouri M, Emmanouilidou E, Rideout H J and Stefanis L 2011 Pathological roles of α -synuclein in neurological disorders *Lancet Neurol.* **10** 1015–25
- [52] Liu N, Zhu L Q, Feng P, Wan C J, Liu Y H, Shi Y and Wan Q 2015 Flexible sensory platform based on oxide-based neuromorphic transistors *Sci. Rep.* **5** 18082
- [53] Smith J T, Shah S S, Goryll M, Stowell J R and Allee D R 2014 Flexible ISFET biosensor using IGZO metal oxide TFTs and an ITO Sensing Layer *IEEE Sens. J.* **14** 937–8
- [54] Jeon J-H and Cho W J 2019 Silicon-on-insulator double-gate ion-sensitive field-effect transistors using flexible paper substrate-based extended gate for cost-effective sensor applications *J. Nanosci. Nanotechnol.* **19** 6668–74
- [55] Park J-S, Jeong J K, Chung H J, Mo Y-G and Kim H D 2008 Electronic transport properties of amorphous indium–gallium–zinc oxide semiconductor upon exposure to water *Appl. Phys. Lett.* **92** 072104
- [56] Lee S and Jeong J 2019 Electrical stability of solution-processed a-IGZO TFTs exposed to high-humidity ambient for long periods *IEEE J. Electron Device* **7** 26–32
- [57] Lilja H, Ulmert D and Vickers A J 2008 Prostate-specific antigen and prostate cancer: prediction, detection and monitoring *Nat. Rev. Cancer* **8** 268–78
- [58] Reyes P I, Ku C J, Duan Z, Lu Y, Solanki A and Lee K B 2011 ZnO thin film transistor immunosensor with high sensitivity and selectivity *Appl. Phys. Lett.* **98**
- [59] Lee J, Dak P, Lee Y, Park H, Choi W, Alam M A and Kim S 2014 Two-dimensional layered MoS₂ biosensors enable highly sensitive detection of biomolecules *Sci. Rep.* **4** 7352
- [60] Rani D, Pachauri V, Madaboosi N, Jolly P, Vu X-T, Estrela P, Chu V, Conde J P and Ingebrandt S 2018 Top-down fabricated silicon nanowire arrays for field-effect detection of prostate-specific antigen *ACS Omega* **3** 8471–82
- [61] Huang Y-W, Wu C-S, Chuang C-K, Pang S-T, Pan T-M, Yang Y-S and Ko F H 2013 Real-time and label-free detection of the prostate-specific antigen in human serum by a polycrystalline silicon nanowire field-effect transistor biosensor *ACS Anal. Chem.* **85** 7912–8
- [62] Lue C-E, Wang I S, Huang C H, Shiao Y-T, Wang H-C, Yang C M, Hsu S H, Chang C Y, Wang W and Lai C S 2012 pH sensing reliability of flexible ITO/PET electrodes on EGFETs prepared by a roll-to-roll process *Microelectron. Reliab.* vol 52 (Amsterdam: Elsevier) pp 1651–4